SIGNIFICANCE OF SPACE CHARGE AND THE EARTH MAGNETIC FIELD ON THE DISPERSIVE CHARACTERISTICS OF A LOW ENERGY ELECTRON BEAM

R. A. Kishek[@], G. Bai, S. Bernal, T.F. Godlove, I. Haber, P.G. O'Shea, B. Quinn, M. Reiser, C. Tobin, M. Walter,
Institute for Research in Electronics & Applied Physics, University of Maryland, College Park, MD

Abstract

The combination of energy spread and space charge provides a rich domain for interesting beam dynamics that are currently not well understood. The University of Maryland Electron Ring (UMER) [1] is a small scaled ring designed to probe the little-known regions of higher beam intensities using low-energy electrons. As such, design, commissioning and operation of UMER present many challenges, some quite novel. For example the UMER beam energy of 10 keV makes the beam very sensitive to the Earth magnetic field, which we can fortunately use to assist in bending the beam. This paper presents a systematic simulation study of the interaction of space charge and energy spread, with and without the earth magnetic field.

INTRODUCTION

The effects of energy spread on beams without significant space charge have long been understood [2]. Emerging accelerators such as spallation neutron sources, future colliders, and heavy ion fusion machines, however, contain significant space charge which will affect the beam dynamics differently in the presence of an energy spread. This has been of some concern to the University of Maryland Electron Ring (UMER) [1], which is designed to model high-intensity ion machines in a dispersive lattice using low-energy (10 keV) electrons. This concern led to the development of the first accurate analytical model of dispersive effects with space charge [3], which was validated to some extent by computer simulation [4]. This effort demonstrated that for the energy spread previously anticipated for the UMER beam (up to 50 eV), the effects of dispersion are of little consequence.

Recent experiments confirming an anomalous growth in energy spread due to space charge modes [5] resulted in a renewed interest in energy spread effects. While these modes have been predicted by simulations long ago [6], this is the first experimental observation. This means that the energy spread of the UMER beam, measured to be less than 20 eV near the source, can in principle, at least, grow to values well above that as a result of space charge effects. This in turn can make issues like dispersion and chromaticity much more significant.

@ ramiak@umd.edu

This study systematically applies the 2.5-D version of the particle-in-cell code WARP [7] to reexamine the role of energy spread in intense beams. Of particular interest here is not only the extreme intensity regime near the space charge limit that was investigated in Ref. [4], but also the intermediate regimes where space charge is abundant but not necessarily dominant. A unique feature of low-energy electron machines such as UMER is their susceptibility to the earth magnetic field, which can significantly alter the local bending radius of the beam. We thus also assess the significance of the Earth field to the dispersive characteristics of the UMER beam.

COMPUTATIONAL MODEL

The UMER lattice is a FODO design with a lattice period length of 32 cm. Each lattice period contains one 10° bend, requiring 36 periods to complete the ring, thus resulting in a circumference of 11.52 m. For this study, we fixed the quadrupole strength at 7.78 and 7.75 G/cm for the F and D quads, respectively, where the effective length of the quads is 3.691 cm. The slight asymmetry is needed to compensate for that introduced by the dipoles. The dipole strength is about 15.37 Gauss, but is reduced to almost 12 G if we impose a 0.4 G vertical component of the Earth magnetic field, since the dipole effective length of 3.86 cm is much shorter than a lattice period. We use hard-edge magnet models throughout in this paper to simplify the results and isolate the effects of energy spread. More details on the UMER lattice and beams can be found in Ref. [1].

Using the above numbers, the zero-current tune is ν_o = 7.7, for which value and the average UMER radius of 1.83 m, one calculates an average dispersion function $D_e = R/\nu_o^2 = 0.031$ m. According to [3], this dispersion function will be significantly modified by space charge. Chromaticity for these parameters is predicted to be $\xi* = \Delta\nu_o/\delta = -11.1$. For comparison, we run all tests for three different levels of energy spread: 1 eV (negligible), 20 eV (measured), and 200 eV (unrealistic upper limit). These numbers correspond to longitudinal momentum spreads $\delta = \Delta p_z/p_{zo} = 5\cdot10^{-5}$, 0.001, and 0.01, respectively. UMER currently uses no sextupole for correction, though one can be added if necessary. To examine space charge effects, we run three sets of cases: zero-current (a nanoAmp, actually), 0.6 mA / 4 μm emittance and 24 mA / 30 μm emittance beams. The last two are consistent with actual beams used in UMER experiments, and correspond to space charge tune depressions ν/ν_o of 0.75 and 0.27, respectively. Where the Earth field is applied, the beam is initially displaced by 0.5 mm (16 cm away from the center of the 1st dipole) so as to have a closed-orbit with minimum centroid displacement.

Simulations are run with adequate numerical parameters, such as 256x256 cells across a 5x5 cm box, 100,000 particles with Gaussian filtering, and 1 mm steps. The transverse gridding is further refined for the 0.6 mA beam due to the tiny beam size, but both the gridding and number of particles are much more relaxed for the zero-current beam since the field solver is turned off completely. All parameters used have been adequately tested. All simulations are started with a semi-Gaussian distribution (uniform in space, Gaussian with uniform temperature in velocity space).

RESULTS

Figure 1 is the dispersion function over the first 10 turns calculated from the simulation using the formula $\langle x\delta\rangle/\langle\delta^2\rangle$ [4], where <…> refers to the moment of the enclosed quantity over the distribution of all particles in the beam. Note that the initial oscillations are damped by phase mixing from the energy spread, and in the 24 mA case, damped even faster by space charge. For no space charge (the black curve), the final average value of the dispersion function is about 0.032, well in agreement with the theoretical prediction. An increase in space charge leads to an increase in the dispersion function, by as much as a factor of 4 for the 24 mA beam (green).

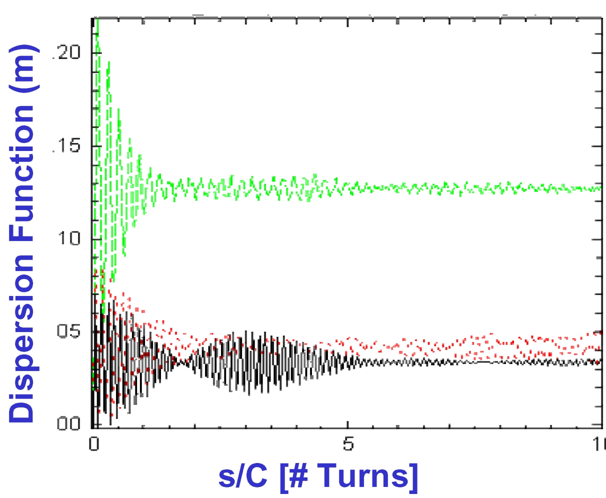

Fig. 1: Dispersion function for the 0 [black], 0.6 [red], and 24 [green] mA beams, for the δ=0.01 case.

Despite this large dispersion, the beam size is not affected as much for the space-charge-dominated beams, as seen in Fig. 2(a). Here, the rms beam radius for the same three cases is plotted. Note that the beam most affected is not the most intense the more intermediate 0.6 mA beam (red), which grows 30% in size. This is the case because space-charge-dominated beams are less sensitive to emittance variations, as the beam size is determined primarily by the tremendous potential well exerted by the beam self-fields. The rms emittances, plotted in Fig. 2(b) show a comparable increase in all 3 cases, again with the 0.6 mA case seemingly with the largest relative increase, with almost 70% growth in emittance. Note however that in the two low-space charge cases, only the x-emittance increases, as predicted by theory; whereas in the 24 mA case (green), the increase in the x emittance is arrested by an exchange of energy with the y direction, leading to a similar growth in the y emittance. This effect and the mechanism behind it were discussed at length in Ref. [8]. Thus the emittance in each direction grows by 30-35%. Noteworthy in both plots is the much faster damping in the case of the 24 mA beam.

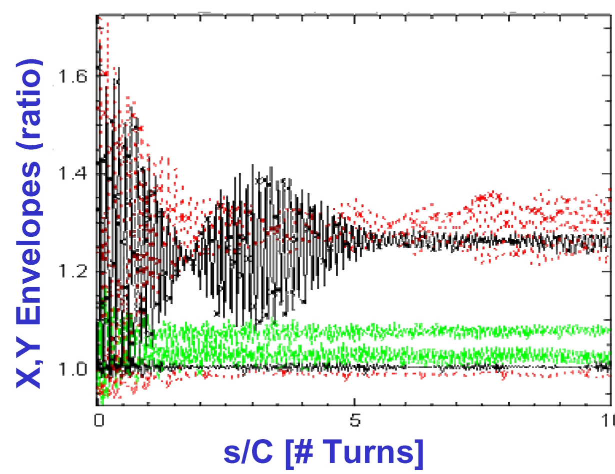

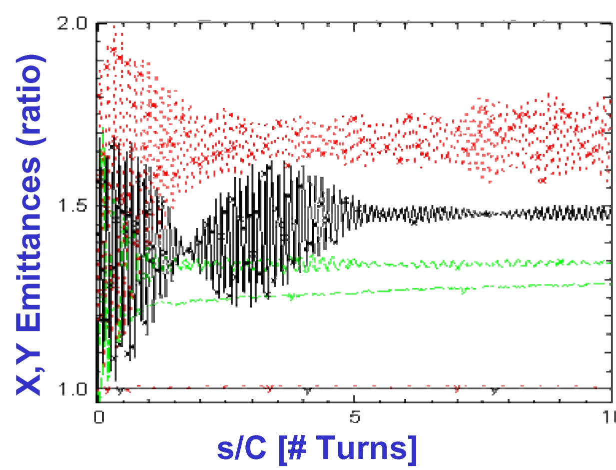

Fig. 2: (a) rms beam radius, and (b) rms emittance for the same three cases in Fig. 1.

The above figures resulted from simulations assuming an unrealistic 200 eV energy spread, exaggerated to make dispersive effects measurable. Looking at smaller, more realistic, energy spreads, the effects are not so obvious. For example, for the 0.6 mA beam, shown in Fig. 3 on a much longer time scale, almost no effect is seen for the 20 eV energy spread (here in red). For the 200 eV energy spread (green), as before the effect is substantial,

0-7803-8859-3/05/$20.00 ©2005 IEEE

resulting, after the initial damping from the energy spread, in a mismatch that persists for 50 turns and more.

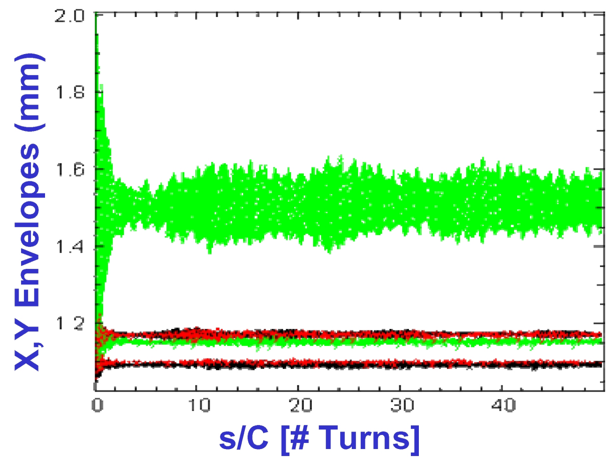

Fig. 3: 2*rms beam radii for δ=5e-5 [black], 0.001 [red], and 0.01 [green] velocity spreads, and I=0.6 mA.

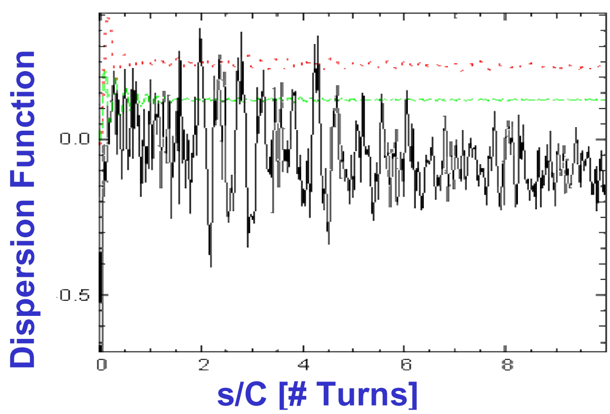

Fig. 4: Dispersion function for δ=5e-5 [black], 0.001 [red], and 0.01 [green] velocity spreads, and I=24 mA.

A particularly intriguing result is the dependence of the dispersion function on energy spread when space charge is significant, as seen in Fig. 4 for the 24 mA beam. This dependence is not seen for the lower-current cases, where the dispersion function is very near similar regardless of energy spread. Even more remarkable is the nonlinear effect whereby the dispersion function is largest for intermediate energy spreads, such as the 20 eV expected for UMER. For some reason this is not reflected in the emittance growth, which is larger for the higher energy spreads as we intuitively expect. This reduction in the dispersion function likely results from the rapid emittance growth and damping in that high-current, high-energy-spread case. One can say the beam is redistributing in a way to reduce the dispersion function. A better understanding of this is a ripe topic for further research.

Finally, a note on the addition of the earth magnetic field. Though the earth field considerably affects the steering of the beam and has created difficulties in injection [9], apparently from these simulations it plays little role on dispersion. For the 0.6 mA beam, the dispersion function is completely unaffected. This can be explained by remembering that though the earth magnetic field changes the local radius of curvature, the average radius remains unaffected. However, as seen from Fig. 5, there is a slight increase in emittance, which perhaps occurs from the combination of energy spread, space charge, and centroid displacement [10].

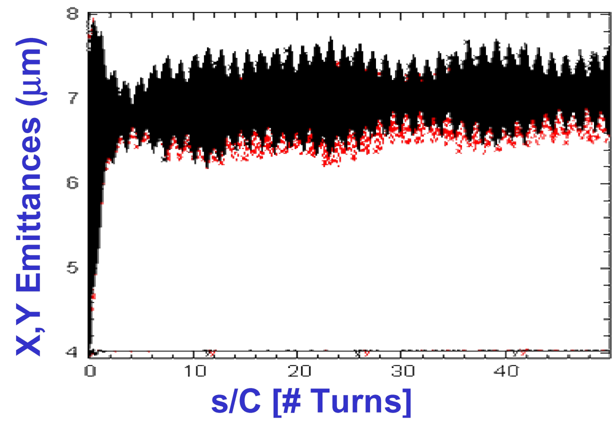

Fig. 5: Effective unnormalized emittance with (black) and without (red) the Earth field for I=0.6 mA and δ=0.01.

In conclusion, this study points to the many interesting issues that result when space charge and dispersion are both present. Much more analysis can be done with this data including a quantitative comparison with Venturini's and Barnard's theories as well as analysis of chromaticity effects. There is no space here to discuss the changes to the beam phase space, which is quite interesting, as well as the effects of injection. All this will appear in a later publication.

We thank Dave Grote and Alex Friedman for their excellent support of the WARP code. This work is funded by US Dept. of Energy grant numbers DE-FG02-94ER40855 and DE-FG02-92ER54178.

[1] S. Bernal, *et al.*, these proceedings.
[2] Martin Reiser, Theory and Design of Charged Particle Beams, (New York: John Wiley & Sons, Inc., 1994).
[3] M. Venturini and M. Reiser, Phys. Rev. Lett., **81**, 96 (1998).
[4] M. Venturini, R.A. Kishek, and M. Reiser, Proc. Workshop on Space-Charge Physics in High Intensity Hadron Ring at Shelter Island, NY, 1998, (New York: AIP Press, no. 448, 1998), p. 278.
[5] Y. Zou, Y. Cui, M. Reiser, and P. G. O'Shea, Physical Review Letters **94**, 134801 (2005).
[6] I. Haber, D. A.. Callahan, A. Friedman, D. P. Grote, and A.B. Langdon, Fusion Engineering & Design, **32-33**, 169-174 (1996).
[7] D.P. Grote, A. Friedman, I. Haber, S. Yu, Fus. Eng. & Des. **32-33**, 193-200 (1996).
[8] R. Kishek, P.G. O'Shea, and M. Reiser, Phys. Rev. Lett., **85** (21), 4514 (2000).
[9] M. Walter, *et al.*, these proceedings; G. Bai, *et al.*, these proceedings.
[10] J.J. Barnard, J. Miller, and I. Haber, Proc. PAC '93, p. 3612 (1993).